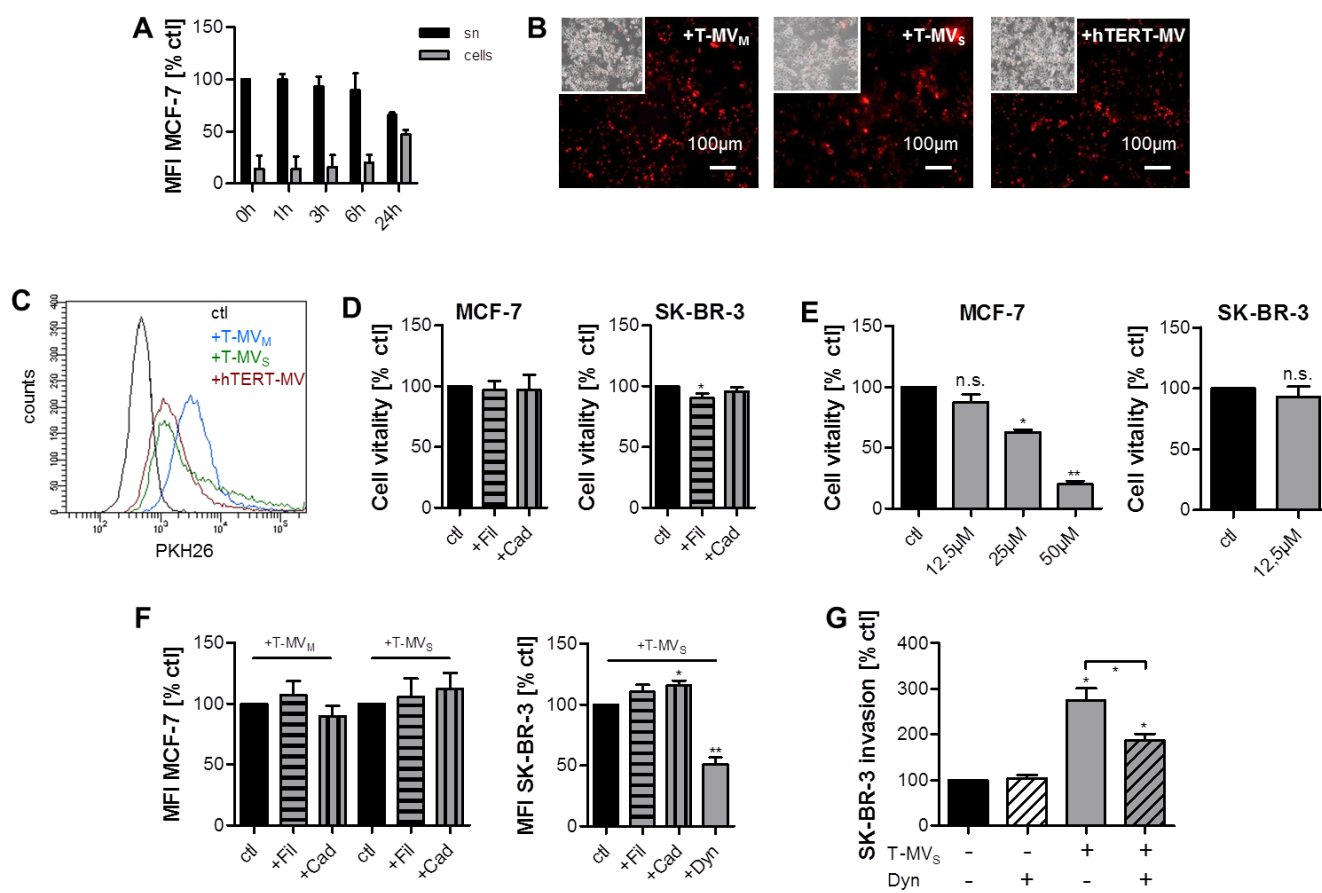


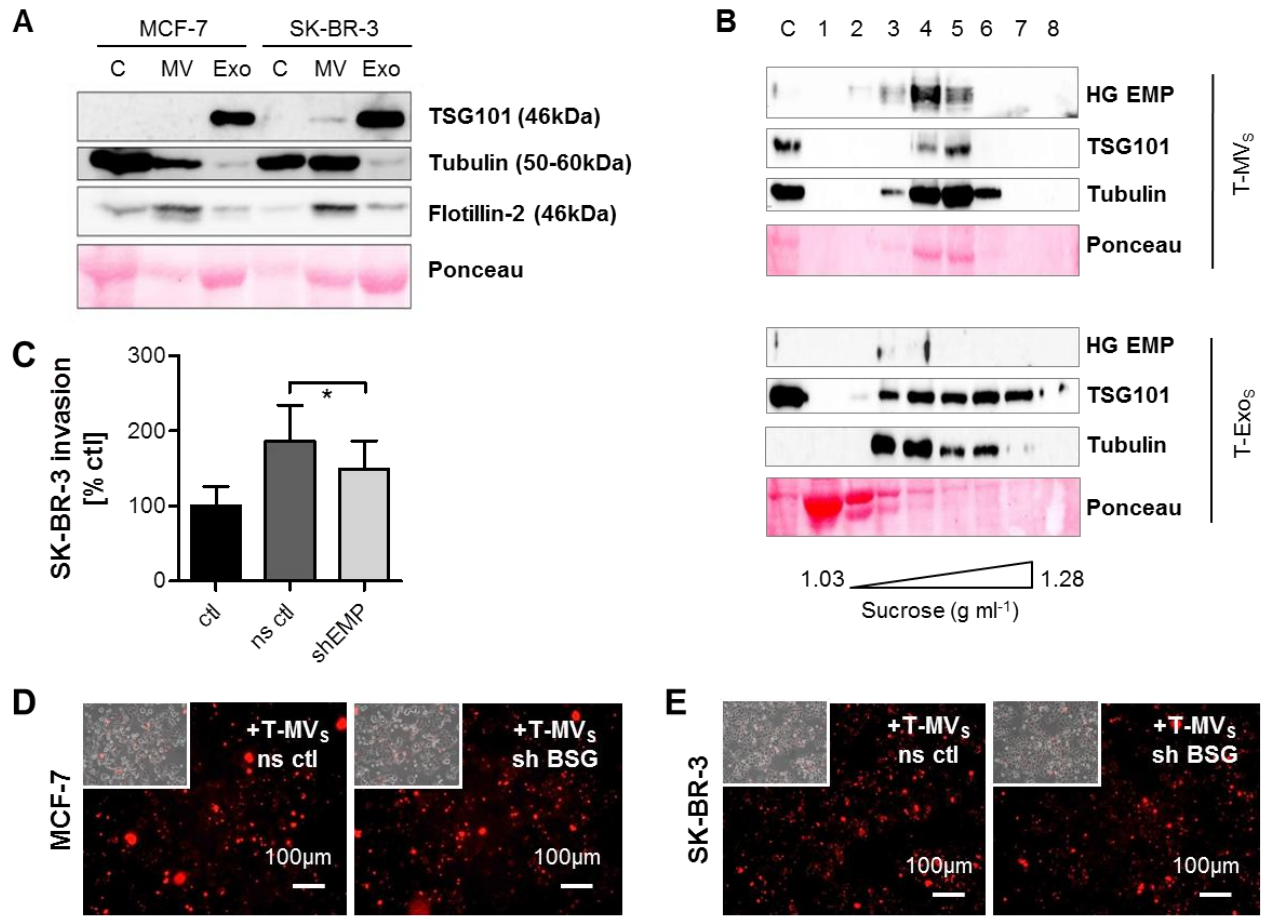
Supplementary Figure S1: T-MV enhance cancer cell invasion.

A, SK-BR-3 cells were stimulated with T-MV and T-Exo (1 μg/ml) or vesicle-free supernatants (sn, 1:3) for 96 h in a modified Boyden chamber (mean±SD, n=3, *p<0.001, **p<0.05). Suffix _M: vesicles/supernatant from MCF-7 cells, _s: SK-BR-3, _{MDA}: MDA-MB231. **B**, Microinvasion assay of MCF-7 cells stimulated with increasing concentrations of T-MV (mean±SD, n=3, *p<0.05, **p<0.001). **C**, MCF-7 cells were seeded in Matrigel-coated 24-well plates, stimulated with T-MV_M (10 μg/ml) and incubated for 96 h. Changes in cell proliferation were determined by cell counting (mean±SD, n=3). **D+E**, xCELLigence proliferation assays for both MCF-7 and SK-BR-3 cells stimulated for 96 h with T-MV (10 μg/ml).



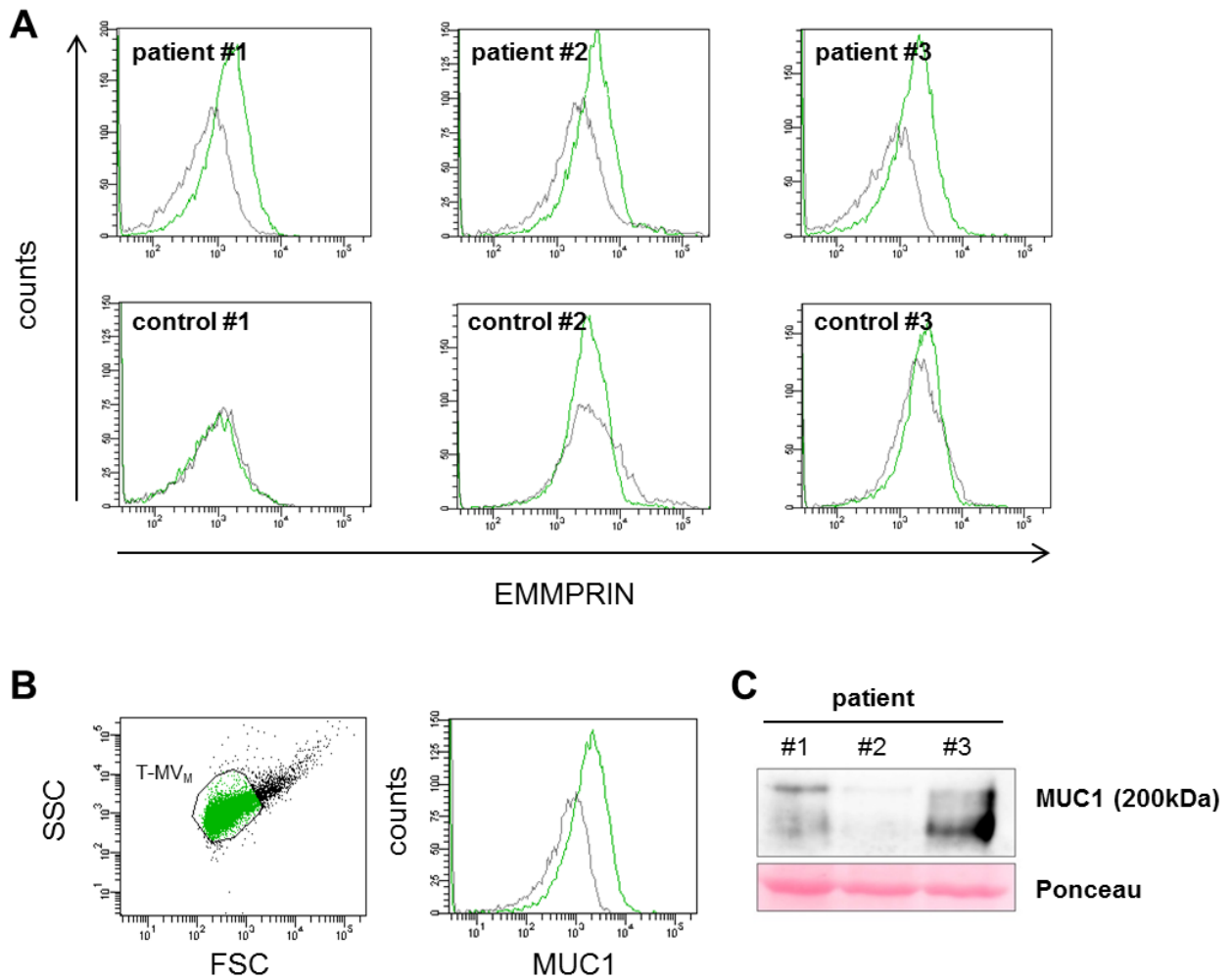
Supplementary Figure S2: MV uptake into breast cancer cells.

A, MCF-7 cells were stimulated for the indicated time periods with 5 μg PKH26-labeled T-MV_M and the red fluorescence in the cells and supernatant (sn) was quantified by flow cytometry. **B**, SK-BR-3 cells were incubated for 24 h with PKH26-labeled MV (5 $\mu\text{g}/\text{ml}$) and uptake was investigated by fluorescence microscopy (magnification: 10 x, inserts: bright fields). **C**, Uptake of different PKH26-labeled MV populations into MCF-7 cells was quantified after 24 h of stimulation using flow cytometry. Depicted is an overlay of representative histograms of the stimulated tumor cells compared to the unstimulated control. **D+E**, MCF-7 and SK-BR-3 cell vitality upon treatment with 1.25 μM filipin III (Fil) and 25 μM dansylcadaverine (Cad) for 24 h (**D**) or dynasore at the indicated concentrations for 48 h (**E**) (mean \pm SD, $n=3$, * $p<0.05$, ** $p<0.001$). **F**, MCF-7 and SK-BR-3 cells were pre-treated with Fil (1.25 μM), Cad (25 μM) or dynasore (Dyn, 12.5 μM) and uptake of PKH26-labeled MV was quantified by flow cytometry (mean \pm SD, $n=3$, * $p<0.05$, ** $p<0.01$). **G**, Microinvasion assay of SK-BR-3 cells pre-incubated with dynasore and stimulated with T-MV_S (mean \pm SD, $n=3$, * $p<0.001$).



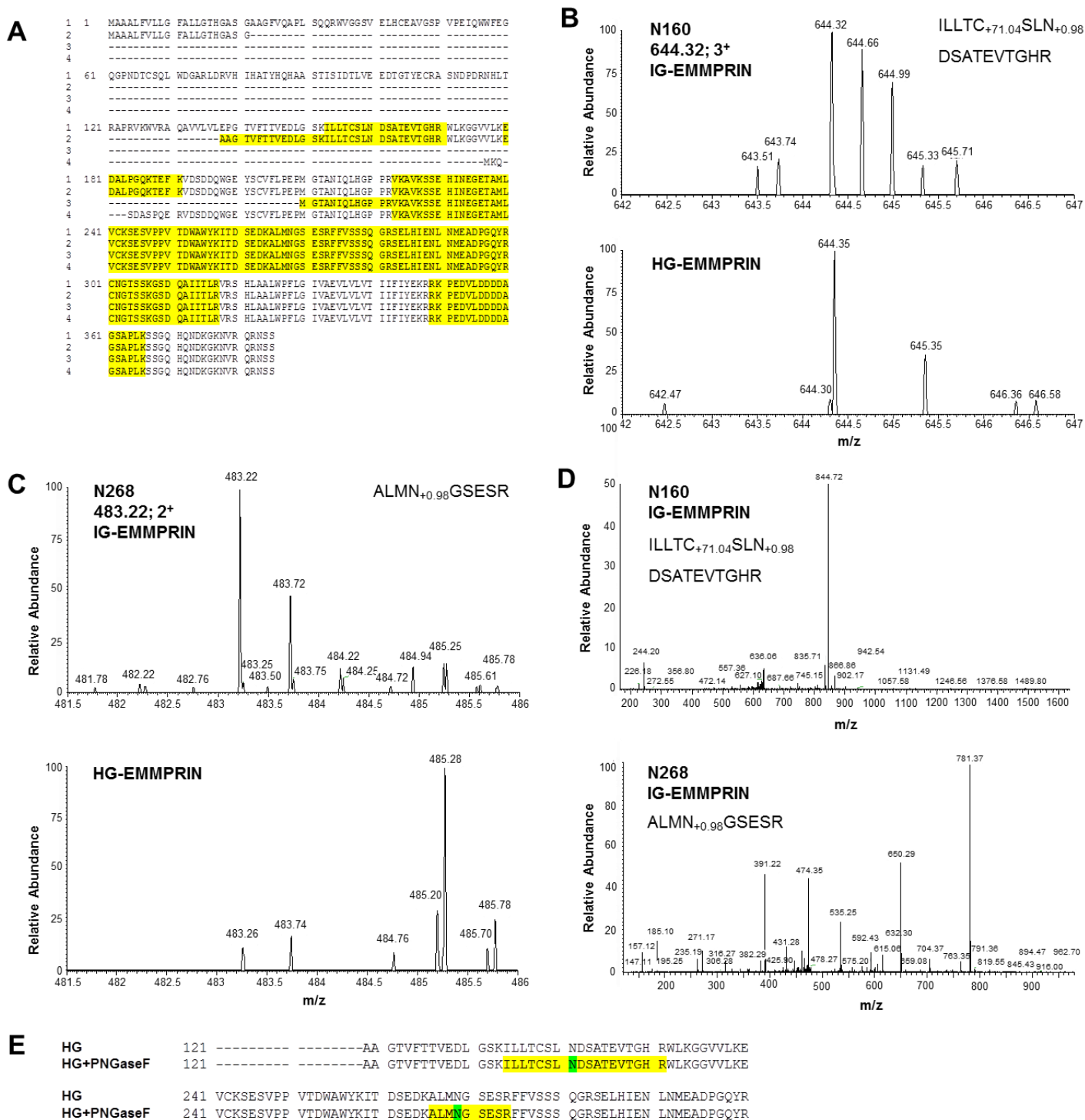
Supplementary Figure S3: EMMPRIN on T-EV.

A, Characterization of T-MV and T-Exo preparations by Western Blotting. **B**, T-MV and T-Exo were loaded separately onto sucrose gradients and the obtained eight fractions were subsequently analyzed by Western Blotting for the established vesicle markers. The whole cell lysate (=C) is shown as comparative control. **C**, Microinvasion assay of SK-BR-3 cells stimulated with T-MV_s (1 µg/ml) from SK-BR-3 EMMPRIN knockdown (shEMP) or non-sense control (ns ctrl) cells (mean±SD, n=3, *p<0.05). **D+E**, Uptake of EMMPRIN-negative MV into breast cancer cells: MCF-7 (**D**) and SK-BR-3 (**E**) cells were stimulated for 24 h with PKH26-labeled T-MV_s shEMP or ns ctrl (5 µg/ml) and uptake was assessed by fluorescence microscopy (magnification: 10 ×, inserts: bright fields).



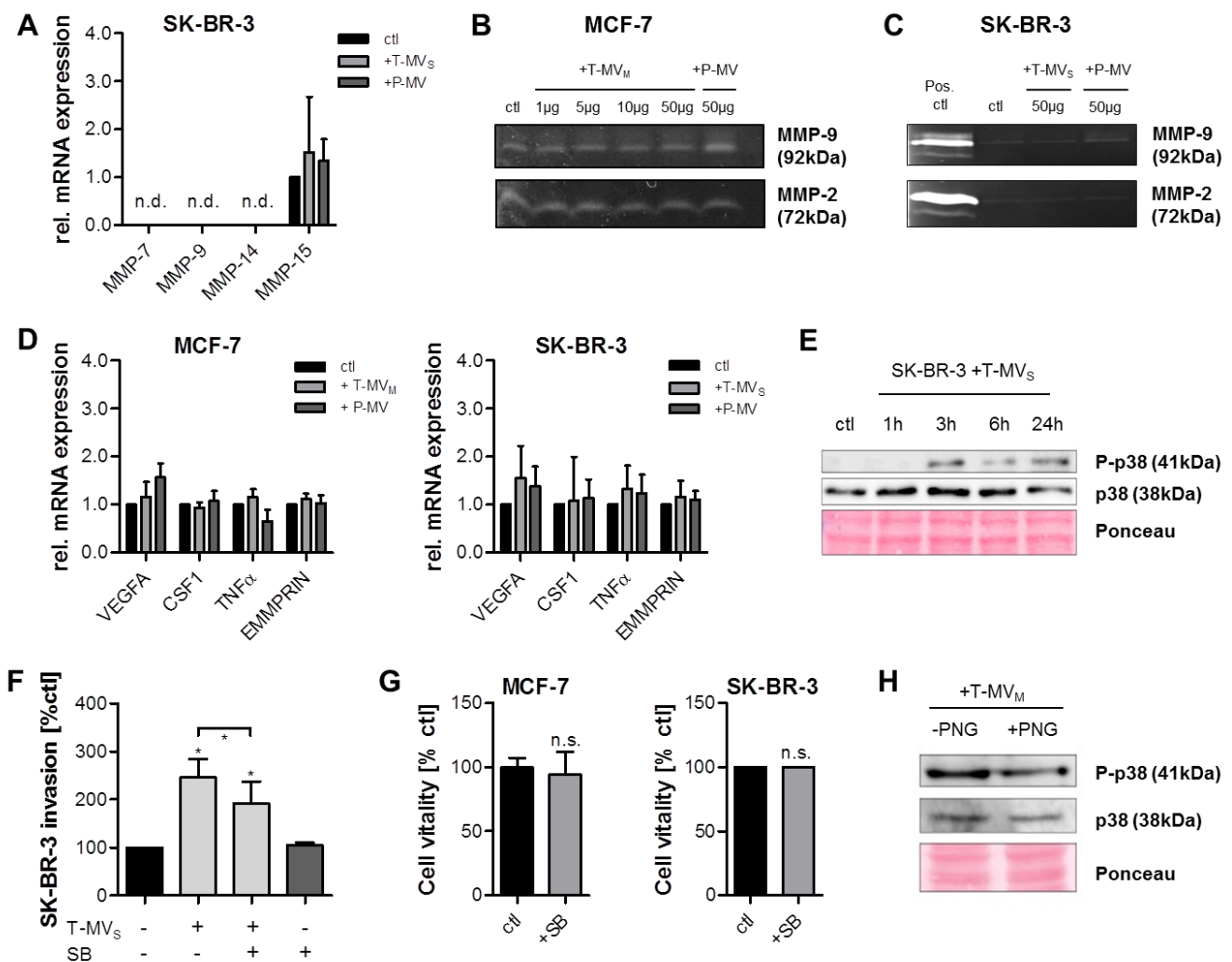
Supplementary Figure S4: EMMPRIN and MUC1 expression on breast cancer patient-derived MV.

A, MV were isolated from breast cancer patients with metastatic disease by differential ultracentrifugation and analyzed by flow cytometry. Histograms represent the EMMPRIN expression on MV (green) from three breast cancer patients and corresponding tumor-free controls. The respective isotype controls are shown in grey. **B**, The expression of the tumor marker MUC1 on T-MV_M was analyzed by flow cytometry. Green: T-MV_M, grey: isotype control. **C**, Additionally, MUC1 expression was determined on patient-derived MV by Western Blotting.



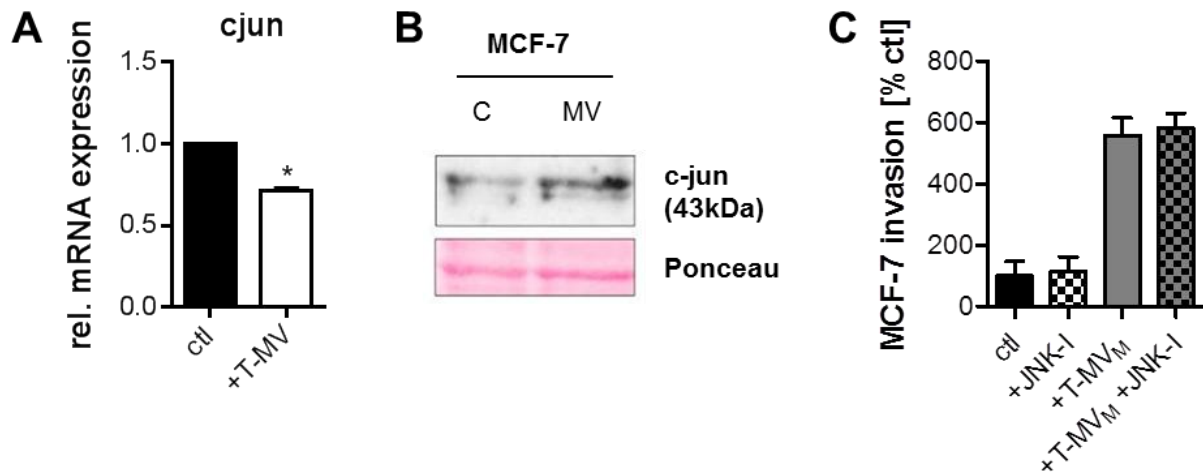
Supplementary Figure S5: LC-MS/MS analysis of IG- and HG-EMMPRIN.

A, Sequence coverage of the EMMPRIN protein in LC-MS/MS analyses. For all four known isoforms of EMMPRIN (1-4), the identified peptides are indicated in yellow. The signal peptide (1-21) or peptides containing the transmembrane domain (324-344) were not found in any sample. **B-D**, Shown are the parent ion masses (**B+C**) as well as the MS/MS spectra (**D**) from the peptides carrying the deamidated N160 or N268 residue which have been recorded on the Orbitrap Velos mass spectrometer in the IG- or HG-EMMPRIN sample. **E**, LC-MS/MS analysis of the HG-EMMPRIN spot +/- PNGaseF. The HG-EMMPRIN (HG) spot was excised from a 1D-gel and analyzed with or without in-gel deglycosylation by PNGaseF. Deglycosylation allows the detection of both peptides (yellow) carrying the two deamidated N-glycosylation sites N160 and N268 (green) which had been absent, and thus glycosylated, in undigested HG-EMMPRIN.



Supplementary Figure S6: Analysis of EMMPRIN target genes.

A, SK-BR-3 cells were stimulated with T-MV for 24 h and cellular MMP expression was assessed by qRT-PCR (mean±SD, n=3, n.d. = not detectable). Stimulation with P-MV was employed as negative control. **B+C**, Zymography of MMP-2 and -9 for MCF-7 (**B**) and SK-BR-3 (**C**) cells incubated with the indicated concentrations of T-MV or P-MV. **D**, MCF-7 and SK-BR-3 cells were stimulated for 24 h with MV (25 µg/ml) and expression of typical EMMPRIN target genes was analyzed by qRT-PCR (mean±SD, n=3). **E**, Phosphorylation of p38 was analyzed by Western Blotting in SK-BR-3 cells after 3 h of treatment with T-MV. **F**, The influence of the p38-inhibitor SB-203580 (SB, 0.5 µM) on the pro-invasive function of T-MV was quantified in microinvasion assays of SK-BR-3 cells (mean±SD, n=3, *p<0.001). **G**, Cell viability assays for MCF-7 and SK-BR-3 cells incubated for 96 h with SB (mean±SD, n=3, n.s.= not significant). **H**, p38 phosphorylation in MCF-7 cells stimulated for 1 h with PNGaseF-treated, deglycosylated T-MV was assessed by Western Blotting.



Supplementary Figure S7: T-MV carry the c-jun protein into breast cancer cells.

A, Expression of c-jun mRNA in MCF-7 cells stimulated with T-MV was quantified by qRT-PCR (mean±SD, n=3, *p<0.05). **B**, Western Blot for the c-jun protein in MCF-7 cells (=C) and MV. **C**, Microinvasion assay of MCF-7 cells pre-treated with a specific JNK inhibitor (JNK-I) prior to stimulation with T-MV (mean±SD, n=3).

Supplementary Table S1: Ingenuity pathway analysis (IPA) of proteins detected on T-MV_M by LC-MS/MS.

Upstream Regulators	p-value	
TP53	5,99E-59	
MAPT	7,58E-39	
MYC	7,95E-35	
APP	4,95E-32	
PSEN1	6,36E-31	

Canonical Pathways		present/total (ratio)
EIF2 Signaling	1,48E-43	84/192 (0,438)
Regulation of eIF4 and p70S6K Signaling	6,42E-29	61/164 (0,372)
Remodeling of Epithelial Adherens Junctions	5,22E-28	41/68 (0,603)
Integrin Signaling	7,77E-25	66/208 (0,317)
mTOR Signaling	2,87E-24	64/198 (0,323)

Molecular and Cellular Functions		# molecules
Molecular Transport	1,24E-29 - 2,91E-05	324
Cellular Growth and Proliferation	6,20E-27 - 2,31E-05	528
Protein Trafficking	4,65E-26 - 1,98E-05	130
Cellular Assembly and Organization	2,61E-25 - 3,35E-05	350
Cellular Functions and Maintenance	2,61E-25 - 3,18E-05	449

Supplementary Table S2: Sequence of primers used for qRT-PCR.

primer	sequence
JUN (hs) forward	5'-CCTTGAAAGCTCAGAACTC-3'
JUN (hs) reverse	5'-CTTTCTGTTTAAGCTGTGCC-3'
BSG (hs) forward	5'-TCACCATCATCTTCATCTACGA-3'
BSG (hs) reverse	5'-GTTCTTGCCTTTGTCATTCTG-3'
BSG-1+2 (hs) forward	5'-GCGAGGAATAGGAATCATGG-3'
BSG-1+2 (hs) reverse	5'-TCTACGGTAGTGAAGACTGTG-3'
BSG-3 (hs) forward	5'-CACAATGAAGCAGTCGGAC-3'
BSG-3 (hs) reverse	5'-TGTCATTCAAGGAGCAGGT-3'
BSG-4 (hs) forward	5'-GAACTTCAAGGGTCCTTCC-3'
BSG-4 (hs) reverse	5'-GAAGACGCAGGAGTACTCTC-3'
GNB2L1 (hs) forward	5'-AACCCATCATCGTCTCCT-3'
GNB2L1 (hs) reverse	5'-CAATGTGGTTGGTCTTCAG-3'
HPRT1 (hs) forward	5'-TATGCTGAGGATTTGGAAAGG-3'
HPRT1 (hs) reverse	5'-CATCTCCTTCATCACATCTCG-3'
MMP7 (hs) forward	5'-CAGATGTTGCAGAATACTCAC-3'
MMP7 (hs) reverse	5'-CACTGTAATATGCGGTAAGTC-3'
MMP9 (hs) forward	5'-ACCTGAGAACCAATCTCAC-3'
MMP9 (hs) reverse	5'-GTAACCATAGCGGTACAGG-3'
MMP14 (hs) forward	5'-GAAGGATGGCAAATTCGTC-3'
MMP14 (hs) reverse	5'-GAGCAGCATCAATCTTGTC-3'
MMP15 (hs) forward	5'-GAGATGTTTCGTGTTCAAGG-3'
MMP15 (hs) reverse	5'-CATGGGATAGTTGTCCAGG-3'
TNF (hs) forward	5'-TCTCTAATCAGCCCTCTGG-3'
TNF (hs) reverse	5'-CTACAACATGGGCTACAGG-3'
VEGFA (hs) forward	5'-CTGAGGAGTCCAACATCAC-3'
VEGFA (hs) reverse	5'-GTCTTGCTCTATCTTTCTTTGG-3'

Supplementary Materials and methods

Cell culture, lentiviral transduction and cell viability

MCF-7, SK-BR-3 and MDA-MB231 human breast cancer cells (ATCC) were grown in RPMI-1640 medium (Gibco) supplemented with 10% heat-inactivated fetal calf serum (FCS, Sigma). Human mammary epithelial cells hTERT-HME1 (Clontech) were cultured in MEGM (Lonza). Human macrophages were differentiated with rhM-CSF (ImmunoTools) from peripheral blood-derived monocytes as described previously (Rietkotter et al., 2013) and maintained in RPMI-1640 with 1% FCS. SK-BR-3 cells with stable knockdown of EMMPRIN were generated through shRNA-mediated gene silencing. Briefly, lentiviral particles were produced in HEK293T cells cotransfected with the packaging plasmids pVSG-G and pCMV Δ R8.91 and the respective TRIPZ shRNAmir plasmid (Thermo Scientific) through calcium phosphate precipitation. While the ns ctrl sequence is proprietary, the EMMPRIN targeting sequence *TCCAAGTTCTCACCTCTTA* (Oligo ID: V3THS_412786) was chosen. The virus-containing supernatant was concentrated using a lentiviral enrichment reagent (MoBiTec) and the titer of the vector preparations determined through flow cytometry. For stable cell line generation cells were transduced with a multiplicity of infection (MOI) of 2 and selected in growth medium containing 2 μ g/ml puromycin (Sigma Aldrich). Gene knockdown was accomplished by addition of 1 μ g/ml doxycycline (Clontech) for 72 h. Cell viability upon treatment with Filipin III (Sigma), Dansylcadaverine (Santa Cruz), Dynasore (Sigma), SB-203580 (0.5 μ M, Calbiochem) or JNK-inhibitor II (5 μ M, Calbiochem) (Klemm et al., 2011) was determined by MTT assay using standard protocols.

LC-MS/MS measurements

Reverse phase separation of tryptic peptides before mass spectrometric analyses was performed on a Proxeon Easy nano-LC system with a binary buffer system consisting of 0.1% acetic acid, 2% acetonitrile in water (buffer A) and 0.1% acetic acid in 100% acetonitrile (buffer B). Peptide separation was achieved using a linear gradient of buffer B from 5 up to 25% within 35 min. MS data were generated using the Orbitrap Velos MS equipped with a nanoelectrospray ion source (PicoTip Emitter, New Objective). After a first survey scan ($r = 60,000$) MS/MS data were recorded for the 20 highest mass peaks in the linear ion trap at a collision-induced energy of 30%. The exclusion time to reject masses was set to 60 s and the minimal ion signal for MS/MS was 2000. For increasing sequence coverage of EMMPRIN and confirmation of deglycosylated peptides (asparagine deamidation) a second LC-MS/MS

analysis was performed using an inclusion list for modified and unmodified parent ion masses (see Supplementary Figures S5B and C).

Mass spectrometry data analysis

Proteins were initially identified by searching against a forward-reverse Swiss-Prot database limited to human entries (v2013-11, n = 38,520, including common contamination sequences) using the SEQUEST algorithm v3.5 (Sorcerer v4.04, Sage-N Research Inc). Search parameters were 10 p.p.m. parent mass tolerance and 0.6 Da for fragment ion mass tolerance. Propionamide modification of cysteins, methionine oxidation and asparagine deamidation were specified as variable modifications. Peptides were annotated on a false positive rate of 0.6% calculated by the Peptide Prophet algorithm. For protein assembling and grouping Trans-Proteomic Pipeline (v4.4.0, Protein Prophet) was used, whereas only proteins with at least two significant peptides were considered for identification and Sequest identifications required at least XCorr scores of greater than 2.5 for double and 3.0 for triple charged ion. Additionally, Scaffold (version Scaffold_4.1.1, Proteome Software Inc) was used to validate MS/MS based peptide and protein identifications. Peptide identifications were accepted if they could be established at greater than 95.0% probability by the Peptide Prophet algorithm (Keller et al., 2002) with Scaffold delta-mass correction. Protein identifications were accepted if they could be established at greater than 95.0% probability and contained at least 2 identified peptides. Protein probabilities were assigned by the Protein Prophet algorithm (Nesvizhskii et al., 2003). Proteins that contained similar peptides and could not be differentiated based on MS/MS analysis alone were grouped to satisfy the principles of parsimony. For detection of the specific glycosylation sites of EMMPRIN an artificial database was used for SEQUEST analysis, whereas all search and annotation parameters were used as described above. The database was build including an additional EMMPRIN-2 isoform without the signal peptide sequence (1-21). The unique T-MV proteins identified by LC-MS/MS (dataset available at www.evpedia.info (Choi et al., 2013; Kim et al., 2013; Choi et al., 2014)) were analyzed using Ingenuity Pathway Analysis (Ingenuity[®] Systems, www.ingenuity.com) to identify potential upstream regulators, canonical pathways and molecular functions. Statistical significance was calculated by Fisher's exact test.

Peptide synthesis and purification

Sequences for the synthetic EMMPRIN blocking peptides are SLNDSATEVTGHRWLK (P-N160) and ALMNGSESRFFVSSS (P-N268) and have been previously published (Sato et al., 2009). For each peptide a random control peptide was created by shuffling the amino acid

sequence resulting in LSDSNGTEAHVTLRWK (P-N160rd) and VFSMELRSNSGFSAS (P-N268rd). Peptides were synthesized using Fmoc solid phase peptide synthesis on a Rink amide MBHA resin (loading density 0.57 mmol/g). For the attachment of the first amino acid the resin was placed in a syringe equipped with a polyethylene-frit (BD) and swollen in DMF for 2 h. For loading the resin, the Fmoc-amino acid (5.0 eq. relative to the resin loading), HOBt (5.0 eq.) and DIC (10 eq.) were dissolved in a minimum of DMF, transferred to the resin and allowed to react using Discover microwave reaction cavity (CEM, 40 °C, 20 W, 10 min). Subsequently, the reaction mixture was filtered and the resin was thoroughly washed with DMF. The loading procedure was repeated twice. Finally, the resin was washed with DMF, NMP and DCM and dried under reduced pressure over night. The resin loading was estimated via UV analysis of the dibenzofulven concentration resulting from Fmoc-deprotection. Therefore, the particular resin (5 mg) was placed in a graduated flask (10 ml) and 2% DBU in NMP was added. After gentle shaking for 1 h, the reaction mixture was diluted with acetonitrile up to 10 ml. The solution was further diluted with acetonitrile (1/12.5) and transferred to a UV cell. The absorption of the cleaved Fmoc species was detected at 304 nm. When the loading density of the resin was considered to be sufficient, the remaining free amino functionalities were acetylated using acetic acid anhydride (1.0 eq.), DIPEA (0.3 eq.), HOBt (0.03 eq.) in NMP (20 eq.) (2 × 10 min). The four peptides were automatically synthesized via SPPS-protocol on a 0.1 mmol scale using the Liberty peptide synthesizer equipped with a Discover microwave reaction cavity (CEM). The Fmoc-protecting group was removed by treatment with 0.1 M HOBt in piperidine/NMP (1/4, v/v). In each coupling an amino acid building block was used in an excess of five equivalents (0.2 M in NMP) and activated with HBTU (4.9 eq.) and HOBt (5.0 eq.) in NMP (0.5 M). As activator base DIPEA (10 eq., 0.5 M in NMP) was used. For the peptide synthesis the following amino acid building blocks were used: Fmoc-Ala-OH, Fmoc-Arg(Pbf)-OH, Fmoc-Asn(Trt)-OH, Fmoc-Asp(OtBu)-OH, Fmoc-Glu(OtBu)-OH, Fmoc-Gly-OH, Fmoc-His(Trt)-OH, Fmoc-Leu-OH, Fmoc-Lys(Boc)-OH, Fmoc-Met-OH, Fmoc-Phe-OH, Fmoc-Ser(tBu)-OH, Fmoc-Thr(tBu)-OH, Fmoc-Trp(Boc)-OH, Fmoc-Val-OH. Cleavage from the solid support was carried out within 3 h using TFA/water/EDT/TIS (94/2.5/2.5/1.0, v/v/v/v). After filtration the filtrate was concentrated under nitrogen-flow and the peptides were precipitated as white solids applying cold diethylether. HPLC analysis was performed using the Pharmacia AKTA purifier (GE Healthcare) with a linear gradient of A (0.1% TFA in H₂O) to B (0.1% TFA in MeCN/H₂O, 4/1, v/v). MN NUCLEODUR columns (RP-C18) were used for protein analysis and

purification. Peptides P-N160, P-N160rd and P-N268 were dissolved in PBS, P-N268rd in PBS + DMSO (1:1000) and employed for microinvasion assays.

Supplementary References

- Choi, D.S., Kim, D.K., Kim, Y.K., et al. (2013). Proteomics, transcriptomics and lipidomics of exosomes and ectosomes. *Proteomics* 13, 1554-1571.
- Choi, D.S., Kim, D.K., Kim, Y.K., et al. (2014). Proteomics of extracellular vesicles: Exosomes and ectosomes. *Mass Spectrom Rev.*
- Keller, A., Nesvizhskii, A.I., Kolker, E., et al. (2002). Empirical statistical model to estimate the accuracy of peptide identifications made by MS/MS and database search. *Anal Chem* 74, 5383-5392.
- Kim, D.K., Kang, B., Kim, O.Y., et al. (2013). EVpedia: an integrated database of high-throughput data for systemic analyses of extracellular vesicles. *Journal of extracellular vesicles* 2.
- Klemm, F., Bleckmann, A., Siam, L., et al. (2011). beta-catenin-independent WNT signaling in basal-like breast cancer and brain metastasis. *Carcinogenesis* 32, 434-442.
- Nesvizhskii, A.I., Keller, A., Kolker, E., et al. (2003). A statistical model for identifying proteins by tandem mass spectrometry. *Anal Chem* 75, 4646-4658.
- Rietkotter, E., Menck, K., Bleckmann, A., et al. (2013). Zoledronic acid inhibits macrophage/microglia-assisted breast cancer cell invasion. *Oncotarget* 4, 1449-1460.
- Sato, T., Ota, T., Watanabe, M., et al. (2009). Identification of an active site of EMMPRIN for the augmentation of matrix metalloproteinase-1 and -3 expression in a co-culture of human uterine cervical carcinoma cells and fibroblasts. *Gynecologic oncology* 114, 337-342.